

Compact Portable QEPAS Multi-gas Sensor

Lei Dong*, Anatoliy A. Kosterev, David Thomazy, Frank K. Tittel

Department of Electric and Computer Engineering, Rice University, 6100 Main Street,
Houston, TX, UAS 77005

ABSTRACT

A quartz-enhanced photoacoustic spectroscopy (QEPAS) based multi-gas sensor was developed to quantify concentrations of carbon monoxide (CO), hydrogen cyanide (HCN), hydrogen chloride (HCl), and carbon dioxide (CO₂) in ambient air. The sensor assembled in a compact package of dimensions 25cm x 25cm x 10cm was designed to operate at atmospheric pressure. The HCN, CO₂, and HCl measurement channels are based on cw, C-band telecommunication-style packaged, fiber-coupled diode lasers, while the CO channel uses a TO can-packaged Sb diode laser as an excitation source. The sensor incorporates rechargeable batteries and can run on batteries for at least 8 hours. It can also operate autonomously or interact with another device (such as a computer) via a RS232 serial port. Trace gas detection limits of 7.74ppm at 4288.29cm⁻¹ for CO, 450ppb at 6539.11 cm⁻¹ for HCN, 1.48ppm at 5739.26 cm⁻¹ for HCl and 97ppm at 6361.25 cm⁻¹ for CO₂ for a 1sec average time, were demonstrated.

Keywords: quartz-enhanced photoacoustic spectroscopy (QEPAS), portable multi-gas sensor, distributed-feedback diode laser, quartz tuning fork, laser spectroscopy, trace gas detection

1. INTRODUCTION

Carbon Monoxide (CO), hydrogen cyanide (HCN), hydrogen chloride (HCl), and carbon dioxide (CO₂) are post-combustion products in aerospace materials used in spacecraft and the international space station environments. Their absence in a post-combustion environment is a reliable indicator for mission specialists (astronauts) that the air quality is below the spacecraft maximum allowable concentrations for airborne contaminants (SMAC values). Therefore, the development of a compact, multi-gas sensor for early fire detection is of considerable interest [1, 2], specifically since targeting of multiple potential fire gases reduces false positives and negatives.

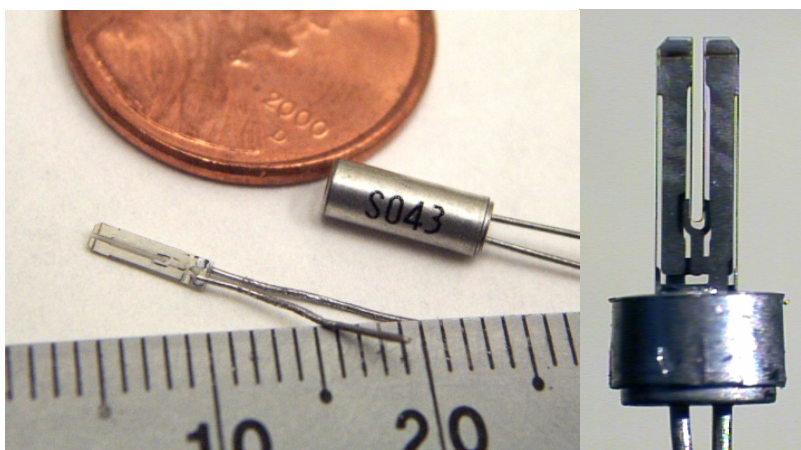


Figure 1. Photograph of quartz tuning forks.

Quartz-enhanced photoacoustic spectroscopy (QEPAS) is based on the use of a quartz tuning fork (QTF) as a

*Lei.dong@rice.edu; phone 1 713 348-5418; fax 1 713 348-5686

detector for acoustic oscillations induced in an absorbing gas by modulated optical radiation [3, 4]. The QTF, as shown in Fig. 1, is a piezo-electric element which converts its deformation into separation of electrical charges. Due to its geometry and arrangement of the electrodes deposited on the quartz crystal (see the right hand side of Fig. 1), the QTF is selectively sensitive to the sound originating in a small, 100-300 μm wide, space between its prongs. In order to enhance the sound signal, an acoustic micro-resonator was employed in most reported QEPAS based gas sensors [5]. It consists of two short pieces of rigid stainless tubing placed along the excitation laser beam direction and positioned close to, but not touching, the QTF, with 30-50 μm gaps. Such a micro-resonator will increase the QEPAS detection sensitivity up to 30 times higher than a bare QTF. The QEPAS technique allows the analysis of gas samples $\sim 3 \text{ mm}^3$ in volume, results in immunity to environmental acoustic noise, and the QEPAS detection module size matches the size of telecommunications diode lasers so that a QEPAS based sensor can be very compact.

In this paper, we design and perform a compact QEPAS four-gas sensor using near infrared laser diodes for early fire detection in detail. The sensor is specifically designed to detect and quantify concentrations of CO, HCN, HCl, and CO₂ in ambient air.

2. Spectral lines selection for CO, HCN, HCl and CO₂

Figure 2 depicts the spectra of CO, HCN, HCl and CO₂ between 1000-9000 cm^{-1} obtained from the HITRAN08 database. The fundamental and the first two overtones of carbon monoxide are located at 4.7 μm , 2.3 μm and 1.6 μm , respectively. For CO detection, we selected the line at 4288.29 cm^{-1} (2.3 μm) as the optimum target line.

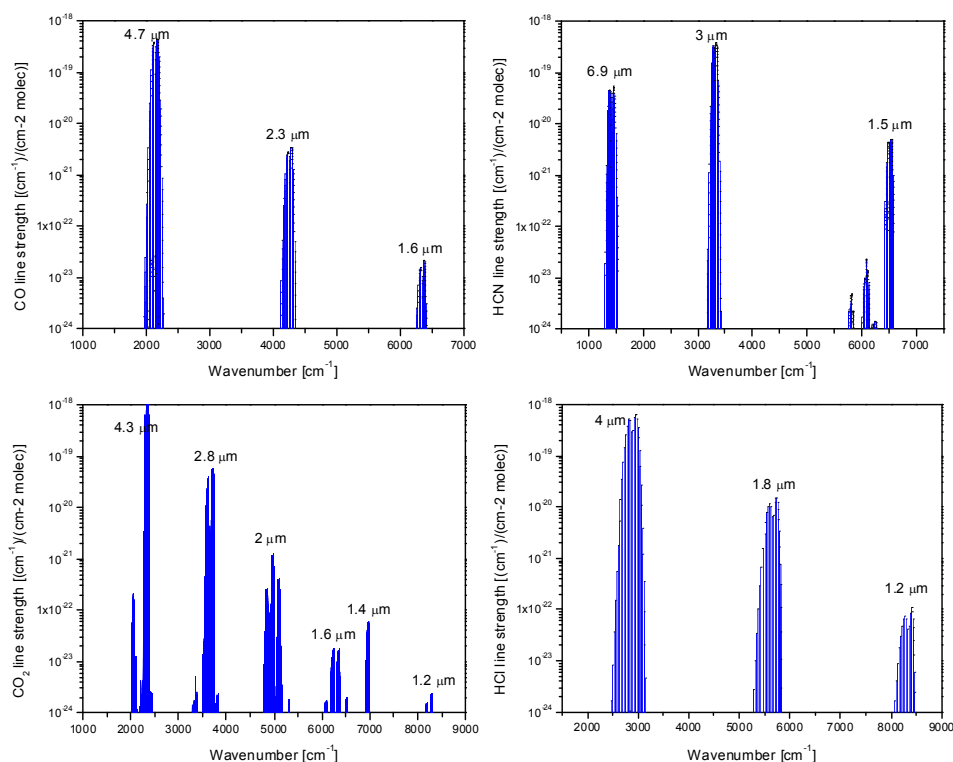


Figure 2. Absorption lines of CO, HCN, HCl and CO₂ between 1000-9000 cm^{-1} .

Carbon dioxide has several rotational-vibrational spectra in the near infrared region. For example, its ν_3 fundamental, $2\nu_3$ and $3\nu_3$ overtone band are located at 4.25 μm , 2.15 and 1.43 μm , respectively; its $2\nu_1+2\nu_2^0+\nu_3$ combination band is located at 1.573 μm ; and its $\nu_1+2\nu_2^0+\nu_3$ combination band is located at 2 μm . Due to the ~ 370 ppm background in ambient air, the CO₂ sensor does not require a high sensitivity. Therefore a line at 6361.25 cm^{-1} (1.57 μm) is used.

The infrared spectra of hydrogen cyanide are located at 6.9 μm , 3 μm and 1.5 μm . The 3 μm band is the ν_3 fundamental band. We selected 6539.11 cm^{-1} (1.529 μm) as the HCN target line due to its strong line strength and the available diode laser output power at 1.5 μm .

HCl detection is possible in the ro-vibrational fundamental band (4 μm), as well as in the first (1.8 μm) and the second (1.2 μm) overtone band. We selected an absorption line located at 5739.26 cm^{-1} (1.742 μm).

3. Design of multi-gas sensor

3.1 CO_2 , HCl and HCN sensing channels

The wavelength of the target lines of CO_2 , HCl and HCN are in the telecommunication spectral range as mentioned above. In this spectral range the diode laser sources are available in a standard 14-pin butterfly package, including an integrated isolator, TEC control, and a single mode fiber pigtail. These features make these diode laser sources extremely convenient and easy to use in our multi-gas sensor design.

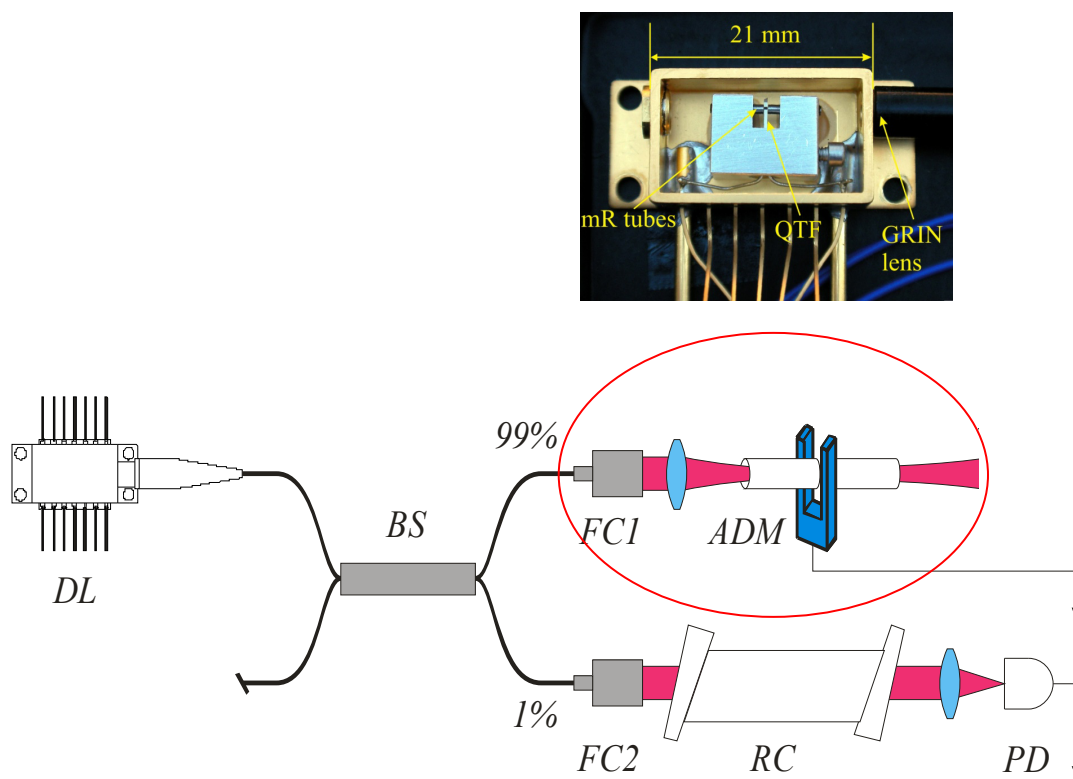


Figure 3. Schematic of a single diode laser sensing channel. DL—diode laser; BS—beam splitter; FC1, FC2—fiber collimator; RC—reference cell; PD—photo detector; ADM—acoustic detection module

The schematic of a single diode laser sensing channel is shown in Fig. 3. The diode laser output is divided in a 1:99 ratio by means of a fiber coupler. 1% of the diode laser light is fiber coupled to a commercial reference module containing a sealed cell filled with a target gas mixture, a fiber collimator, and a photodiode. The remaining laser power is directed to a spectrophone consisting of the QTF and two metal tubes forming the acoustic micro-resonator. The length of each tube is 4.4 mm and the inner diameter is 0.51 mm. The tubes are positioned 0.6 mm below the QTF tips. The spectrophone was placed into an enclosure equipped with a collimator and BK7 window with antireflection coating, as shown in Fig.3 (top). This assembly represents an acoustic detection module (ADM).

3.2 CO sensing channel

The optimum CO absorption line is located at $2.3\ \mu\text{m}$, and at this wavelength a diode laser is only available commercially as a TO5.6 package without a fiber pigtail and TEC control. Hence it was necessary to design a sensing channel that includes discrete components such as a TEC and lens for collimating the diode laser beam to the QTF. In order to make full use of the diode laser power, the TO5.6 can window was removed in order for the focusing lens to be close to the laser chip. The detailed laser assembly is shown in the left hand side of Fig. 4. The complete CO sensing

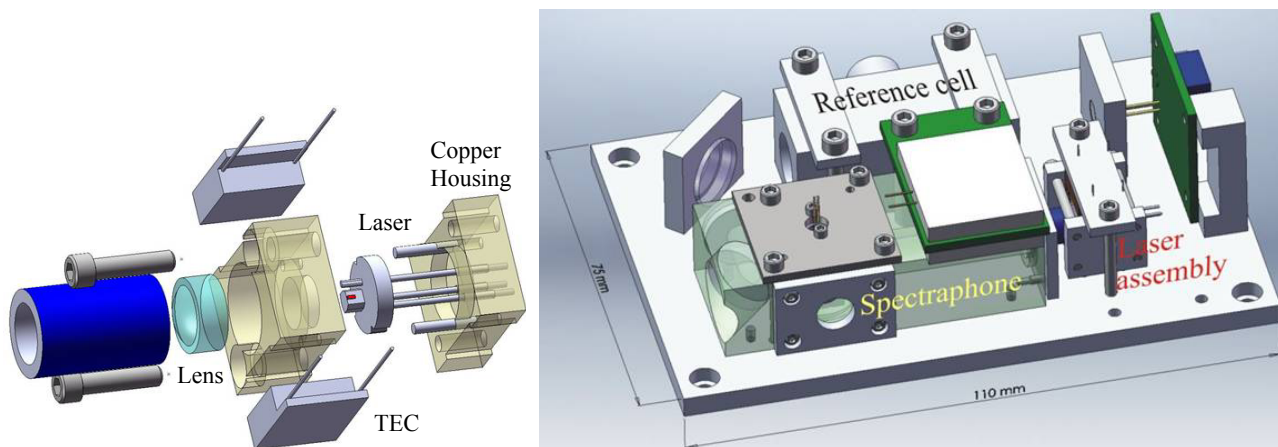


Figure 4. Laser assembly (left); CO sensor (right)

channel is shown on the right hand side of Fig.4, which includes a laser assembly, spectrophone, reference cell and photodetector.

The laser is mounted into a small copper housing. Two small TEC were attached to the wall of the copper housing to control the laser temperature. The coupling lens whose working distance is $1.76\ \text{mm}$ is glued in front of laser housing to focus the output beam between the two prongs of the QTF. The alignment procedure of the diode laser beam is based on precision CNC machining and a passive alignment method. This method reduces significantly labor costs. Furthermore, such a micromechanical approach is suitable for manufacturing large numbers of identical, interchangeable spectrophones. Upon exiting the QTF the laser beam is directed to a reference cell by a 90° reflector and is monitored by a photo detector. The reference signal is used to lock the laser frequency to the CO target line.

3.3 Control electronics unit (CEU) and assembly of a diode laser based QEPAS multi-gas sensor

All the four sensing channels (CO, HCN, HCl and CO_2) are mounted inside the control electronics unit (CEU) with dimensions of $10 \times 25 \times 25\ \text{cm}$, as shown in Fig. 5. The CEU performs the frequency locking functions of the laser wavelengths to the four target absorption lines, as well as measuring the QTF parameters, and modulating the diode lasers at half the resonant frequency of the corresponding QTFs. To determine the QTF parameters, an electrical, sine wave excitation voltage is applied, and the excitation frequency is scanned to determine the QTF natural frequency by measuring the QTF current. The Q-factor was derived from the QTF ringdown time following a sudden interruption of the excitation voltage. Four sets of parameters have been pre-programmed in the CEU, each set includes the selected diode laser, a reference cell, a spectrophone, laser current and temperature, modulation depth, and control parameters. The CEU can be programmed to loop through the desired sets of parameters in an autonomous mode.

Also, the CEU can communicate with an external computer through RS 232, receiving commands and exchanging data. It also includes rechargeable batteries so that the sensor is able to operate on battery power for >8 hours. All 4 ADMs are open cell design. In order to ensure efficient gas exchange between ambient air and the internal sensor case volume, the CEU is equipped with a fan. Therefore, the sensor does not require a vacuum pump, which reduces the overall sensor weight.

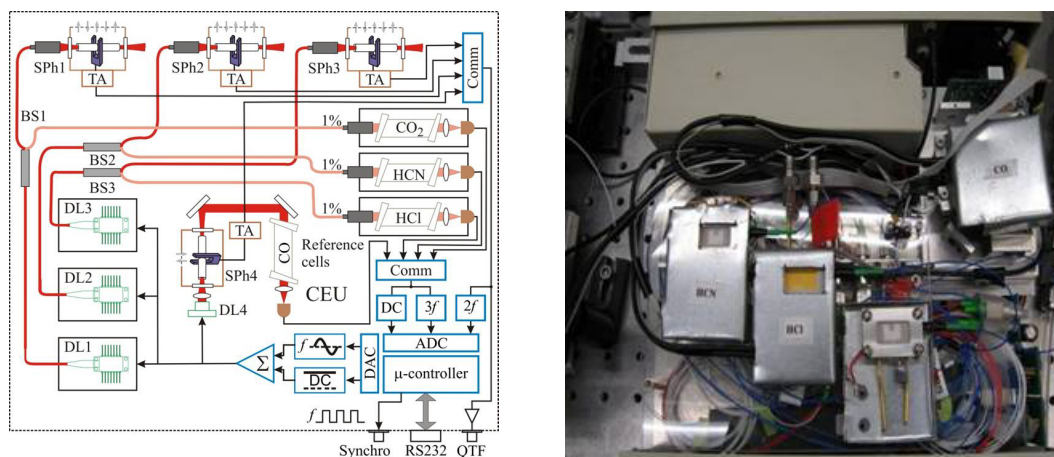


Figure 5. Compact QEPAS multi-gas sensor. Schematic diagram (left); photograph (right). CEU—control electronics unit; DL1, DL2, DL3, DL4—diode lasers; SPh1, SPh2, SPh3, SPh4—spectrophone; TA—transimpedance amplifier

4. Performance assessment of compact multi-gas sensor

4.1 Sensitivity of compact multi-gas sensor

The sensor sensitivity was evaluated in nitrogen as a carrier, using trace gas sources. The results are shown in Table 1.

Table 1. Sensitivity measured in N_2 as a trace gas carrier. All measurements are performed at atmospheric pressure.

Gas	CO	HCN	HCl	CO ₂
Concentration	50 ppm	14 ppm	10 ppm	1500 ppm
Carrier gas	N ₂	N ₂	N ₂	N ₂
Water concentration	1.1%	0%	0%	1.2%
Signal amplitude	835.4 cnt	7883 cnt	2057 cnt	5493 cnt
SNR	6.46	31.07	7	15.42
Noise bandwidth	0.196 Hz	0.785 Hz	0.785 Hz	0.785 Hz
Laser Power	2 mW	35.5 mW	14.7 mW	37 mW
NEC ¹	7.74 ppm	450 ppb	1.48 ppm	97 ppm
NNEA ²	1.41×10^{-8} cm ⁻¹ W/ $\sqrt{\text{Hz}}$	5.3×10^{-9} cm ⁻¹ W/ $\sqrt{\text{Hz}}$	5.17×10^{-8} cm ⁻¹ W/ $\sqrt{\text{Hz}}$	5.73×10^{-9} cm ⁻¹ W/ $\sqrt{\text{Hz}}$

1. NEC: Noise-Equivalent Concentration

2. NNEA: Normalized Noise-Equivalent Concentration.

4.2 Linearity of the sensor response

The linearity of the multi-gas sensor response was evaluated. The results are shown in Fig. 6. A linear response evaluation of the HCl sensor was not performed since only a 10 ppm HCl cylinder was available. The accuracies and linear ranges of the CO, HCN and CO₂ channels were good as shown in Fig. 6.

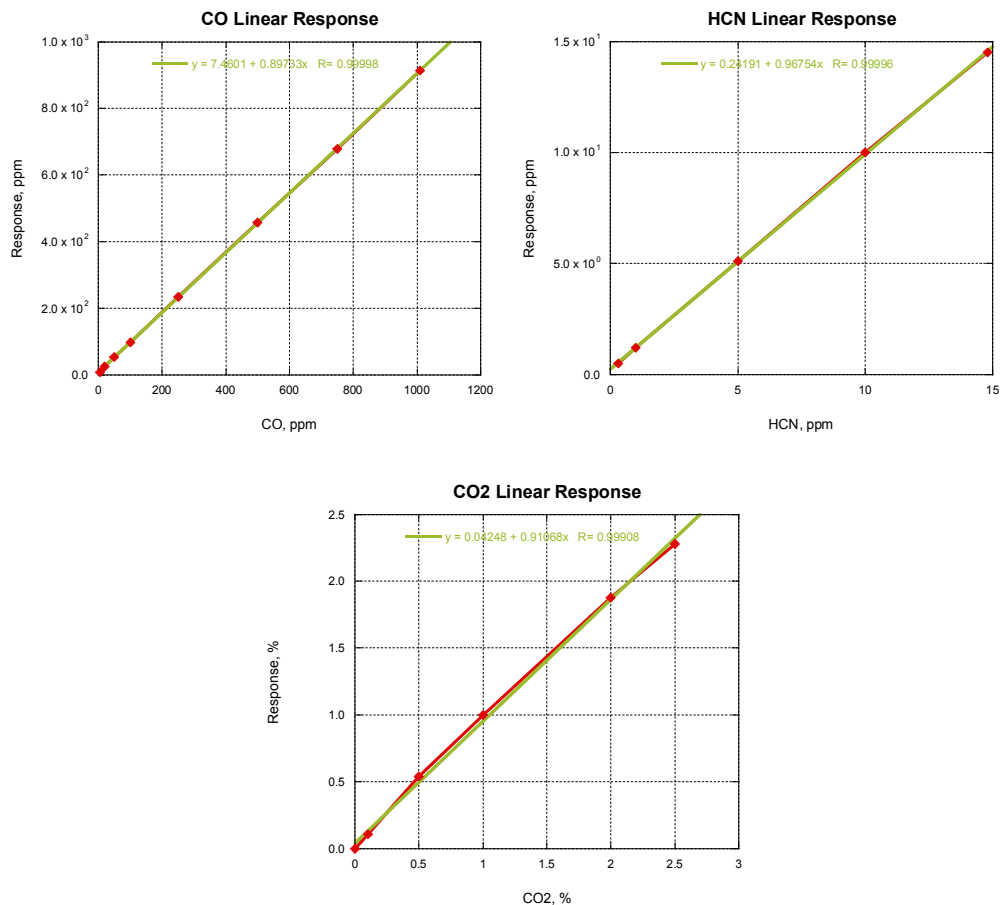


Figure 6. Linear response of CO, HCN and CO₂ sensing channels.

4.3 Gas humidity impact

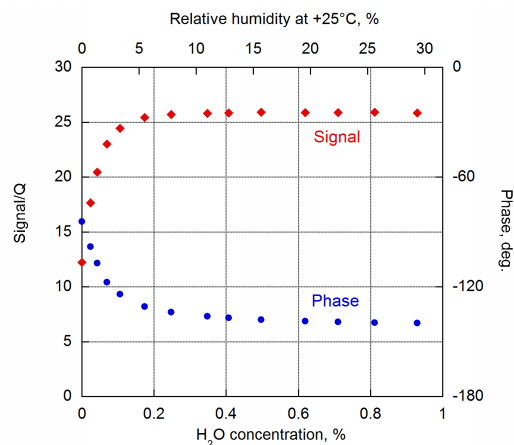


Figure 7. Impact of humidity on CO₂ signal.

In photo acoustic spectroscopy, the vibrational-translational (V-T) relaxation rate of gas plays an important role. In case of a slow V-T relaxation rate with respect to the modulation frequency, the translational gas temperature cannot follow fast changes of the laser induced molecular excitation rate. Thus the generated photoacoustic wave is weaker than it would be in case of instantaneous V-T energy equilibration. However, the presence of H₂O can increase the V-T relaxation rate of the target gas. Figure 7 shows the impact of water vapor on CO₂ signal. When the relative humidity is >0.2 %, the V-T relaxation rate is saturated, and the measured QEPAS signal is no longer impacted by humidity. Similar studies were performed for CO, HCl and HCN. The impact curves are used to calibrate the QEPAS output signals.

4.4 Test data of QEPAS multi-gas sensor

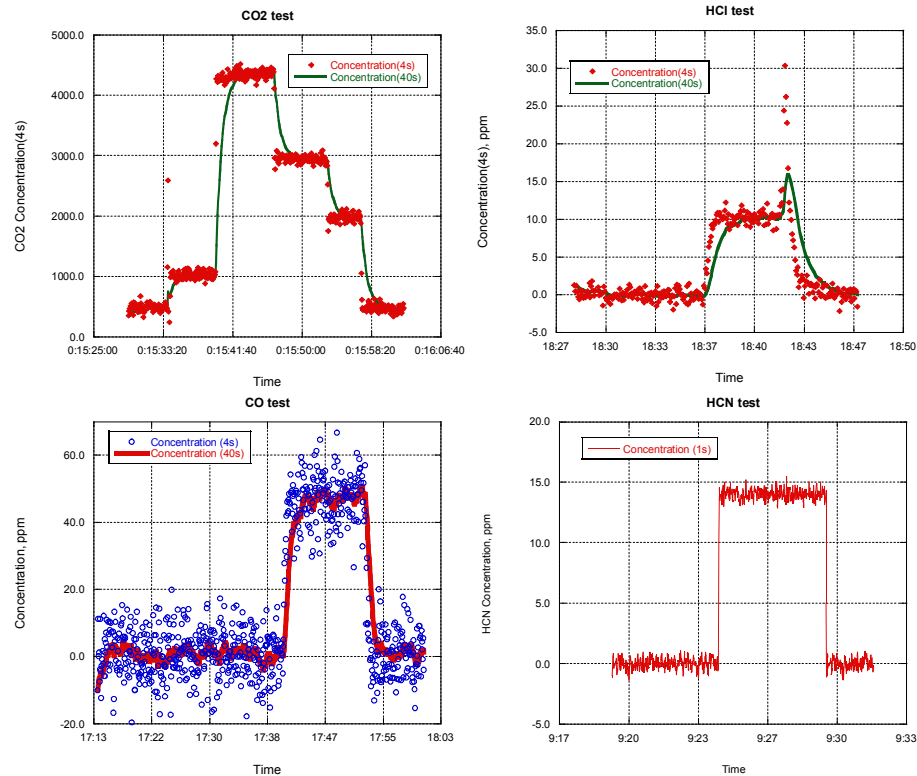


Figure 8. QEPAS signal of compact multi-gas sensor recorded for varied gas concentrations obtained using a commercial gas mixer.

Each of the four sensor channels shows 4-second averaged-response data as discrete dots and a 40-second running average as a solid line. The 4-second averaged-response data can reflect the instantaneous change of the gas concentration, while the 40-second average measures the precise gas concentration. Figure 8 shows the recorded signals while the gas concentration was varied by a gas mixer

5. Summary

In this paper, we designed, assembled, and assessed a compact portable multi-gas sensor, which can quantify CO, CO₂, HCl and HCN simultaneously. We demonstrated detection sensitivity limits (1 s averaging time) of 7.7 ppm for CO, 450 ppb for HCN, 1.5 ppm for HCl and 100 ppm for CO₂, respectively. Our measurements show that the compact, multi-gas sensor based on 3 near-infrared DFB communications and one Sb diode lasers is applicable for early fire detection.

REFERENCES

- [1] A.A. Kosterev, F.K. Tittel and G. Bearman, "Advanced quartz-enhanced photoacoustic trace gas sensor for early fire detection", SAE Int. J. Aerosp. 1, 331-336 (2008).
- [2] D. Thomazy, S. So, A. Kosterev, R. Lewicki, L. Dong, A. A. Sani, F. K. Tittel, "Low-power laser-based carbon monoxide sensor for fire and post-fire detection using a compact Herriott multipass cell", Proc. SPIE 7608, 76080C-76080C-6 (2010).
- [3] A.A. Kosterev, Y.A. Bakhirkin, R.F. Curl and F.K. Tittel, "Quartz-enhanced photoacoustic spectroscopy", Opt. Lett. 27, 1902-1904 (2002)
- [4] A.A. Kosterev, F.K. Tittel, D. Serebryakov, A.L. Malinovsky, I. Morozov, "Application of quartz tuning fork in spectroscopic gas sensing", Rev. Sci. Instr. 76, 1-4 (2005)
- [5] L. Dong, A.A. Kosterev, D. Thomazy, F.K. Tittel "QEPAS spectrophones: design, optimization, and performance", Applied Physics B 100, 627-635 (2010)